Journal of Nanoscience and Nanotechnology
Vol. 7, 1–7, 2007

Structures and Electronic Properties of $M_2C_2@C_{78}$ ($M = Ti, Zr, Hf$): A Density Functional Theory Study

Xin Wu, Xin Lu*, Kai Tan, and Qianer Zhang

Departmental of Chemistry, College of Chemistry and Chemical Engineering, State Key Laboratory of Physical Chemistry of Soild Surface and Center for Theoretical Chemistry, Xiamen University, Xiamen 361005, China

A systematic DFT investigation has been conducted to explore the structures and electronic properties of the metal-carbide endofullerenes $M_2C_2@C_{78}$ ($M = Ti$, Zr, Hf) at the PBE/DNP level of theory. The theoretical calculations predicted the following: (i) this series of endofullerenes have the valence states $[M^{4+}]_2C_2^{2-}@C_{78}^{6-}$; (ii) the structure of the $[M_2C_2]^{6+}$ cluster encapsulated in the $C_{78}^{6-}(D_{3h})$ cage varies with the increasing of the ionic radius of M^{4+}, i.e., from a linear M-C$\equiv$C-M geometry for $M = Ti$, through a zigzag geometry for $M = Hf$ to a side-on binding mode for $M = Zr$; (iii) $M_2C_2@C_{78}$ ($M = Zr$, Hf) should display interesting intramolecular dynamic behavior at room temperature, i.e., the encapsulated C_2^{2-} moiety can rotate freely around the C_3-axis of the $C_{78}^{6-}(D_{3h})$ cage; (iv) the $[Ti_2C_2]^{6+}$ in the lightest $Ti_2C_2@C_{78}$ is far more fixed by adopting the linear Ti-C$\equiv$C-Ti geometry; (v) the order for their ionization potentials is $Ti_2C_2@C_{78} < Hf_2C_2@C_{78} \ll Zr_2C_2@C_{78}$, whereas their EAs follow the order: $Ti_2C_2@C_{78} < Hf_2C_2@C_{78} \approx Zr_2C_2@C_{78}$. The predicted redox properties of these endofullerenes suggest that $Zr_2C_2@C_{78}$ is synthetically as approachable as $Hf_2C_2@C_{78}$.

Keywords: Endohedral Metallofullerene, Metal Carbide, Density Functional, Tetravalent Metals.

1. INTRODUCTION

Endohedral metallofullerenes (EMFs) and their possible applications have attracted much attentions in past two decades.[1] Endohedral metallofullerenes are such a category of fullerene derivatives that encapsulate a metal atom or cluster inside a fullerene cage. Owing to their inherent intramolecular electron transfer from encapsulated atom/cluster to carbon cage, all EMFs so-far discovered have a positively charged endohedral atom/cluster and a negatively charged carbon cage, affording their superatomic nature along with unique physical and chemical properties differing from that of empty fullerenes.[1] The intramolecular electron transfer within an EMF can drastically change the stability of its carbon cage, preferentially giving rise to a negatively charged carbon cage with a *stable close–shell electronic configuration*,[2,3] and in most cases resulting in a stable close–shell electronic configuration for the whole EMF.[4,5] The applicability of the *stable close–shell electronic configuration rule* (CSECR) was exemplified by such EMFs as $Sc_2@C_{66}$,[6] $Sc_3N@C_{68}$,[7] $Sc_2C_2@C_{68}$,[8] and $La_2@C_{72}$,[9] whose carbon cages violate the well-known Isolated Pentagon Rule (IPR) and are extremely unstable in their empty forms.[3a] Recent theoretical and experimental investigations further demonstrated that the close–shell electronic configuration rule (CSECR) is of particular importance for the rational structural determination of EMFs containing two or more metals, e.g., $Ti_2C_2@C_{78}$,[10] $Sc_3C_2@C_{80}$,[11] and $Sc_4C_2@C_{80}$,[12] on account of the limited electron-accepting capacity of fullerene cages (≤ 6)[13] and a relatively larger number of available valence electrons pertaining to the encapsulated metal atoms (normally trivalent or even tetravalent). Note that these two- or multi-metallofullerenes were previously supposed to have the simple endohedral structures $M_m@C_n$ ($M = Ti$, $m = 2$, $n = 80$; $M = Sc$, $m = 3, 4$, $n = 82$).[1,14,15] In this paper, we report the results of our recent density functional theory (DFT) study on the structures of $M_2C_2@C_{78}$ ($M = Ti$, Zr, Hf).

EMFs containing tetravalent metal atoms such as Ti, Zr, and Hf are scarce.[14,16] In 2000, Cao et al. reported the synthesis and characterization of Ti_2C_{80}.[14a] UV-Vis-NIR absorption spectroscopic experiments revealed an optical gap of ~0.88 eV (~1400 nm) for this endofullerene. In addition, a total of 8 ^{13}C NMR signals were disclosed, according to which a mixture of two $Ti_2@C_{80}$ isomers containing correspondingly the I_h- and D_{5h}-symmetric C_{80} cages were proposed.[14a] However, our preliminary DFT calculations[10a] revealed the followings,

(i) the simple endohedral structure $Ti_2@C_{80}$ has an open-shell triplet ground state with two unusual Ti^{3+} cations encapsulated in a C_{80}^{6-} (I_h) cage, inconsistent

---

[*] Author to whom correspondence should be addressed.

1533-4880/2007/7/001/007

doi:10.1166/jnn.2007.313

with the experimentally observation that the $Ti_2@C_{80}$ is diamagnetic;[14]

(ii) a metal-carbide endofullerene structure $Ti_2C_2@C_{78}$ having a D_{3h}-symmetric C_{78} cage is consistent with the experimental ^{13}C NMR spectrum, and, meanwhile, has the formal valence state $[Ti^{4+}]_2[C_2^{2-}]@C_{78}^{6-}$ that perfectly fulfills the CSECR.

A more considerate DFT study by Yumura et al.[10b] further calibrated that the encapsulated $[Ti_2C_2]^{6+}$ cluster favors a linear Ti–C–C–Ti structure (denoted end-on isomer) with the Ti atoms located near the polar hexagons of the D_{3h}-symmetric C_{78} cage. In addition, they found a high-energy $Ti_2C_2@C_{78}$ isomer with a butterfly-like $[Ti_2C_2]^{4+}$ endohedral cluster (denoted side-on isomer) which is by 38.3 kcal/mol higher than the end-on isomer. It is yet unclear whether the $Ti_2C_2@C_{78}$ would show intramolecular dynamic behavior (e.g., rotation of the encapsulated cluster) like that observed for $Sc_2C_2@C_{84}$.[17]

In addition to the synthesis of Ti_2C_{80} (or more exactly $Ti_2C_2@C_{78}$), the synthesis of Hf_2C_{80} was reported by Akiyama et al.[18] This endofullerene has an optical gap of ~0.95 eV (~1300 nm) disclosed by UV-Vis spectroscopic experiments, and was found to be EPR-inactive from 4 K to room temperature by ESR spectroscopy.[18] These phenomena imply a diamagnetic closed-shell electronic configuration for the synthesized Hf_2C_{80}. Accordingly, it is highly probable that the Hf_2C_{80} is isostructural to its congener Ti_2C_{80}, adopting a metal-carbide structure $Hf_2C_2@C_{78}$ to fulfill the CSECR.

Although Zr_2C_{80}, which is congeneric to Ti_2C_{80} and Hf_2C_{80}, has not been synthesized and characterized yet, the encapsulation of zirconium in hollow fullerenes has been confirmed recently by mass spectroscopic experiments.[16] We infer that Zr_2C_{80}, if synthesized, would also be isostructural to its congeneric $Ti_2C_2@C_{78}$.

The aim of the present theoretical work is multifold:

(i) to explore the structures and electronic structures of the congeneric dimetallofullerenes $M_2C_2@C_{78}$ (M = Ti, Zr, Hf);

(ii) to unravel the structures of endohedral clusters as well as their possible intramolecular dynamic behaviors;

(iii) to predict ^{13}C NMR spectrum of $Ti_2C_2@C_{78}$;

(iv) to predict the redox properties (e.g., ionization potential and electron affinity) of these EMFs.

2. COMPUTATIONAL DETAILS

All density functional theory (DFT) calculations were performed with the generalized gradient approximation (GGA) Perdew-Burke-Ernzerhof (PBE) density functional method[19] using the $Dmol^3$ code.[20] For close- and open-shell systems, the spin-restricted and spin-unrestricted algorithms were employed, respectively. All-electron double numerical plus polarization (DNP) basis sets with scalar relativistic corrections[21] on the core electrons, which are of the highest quality among all the available basis sets within the $Dmol^3$ code, were employed for M (M = Ti, Zr, Hf) and C atoms. All structures were optimized at such PBE/DNP level of theory.

The ^{13}C NMR chemical shifts for $Ti_2C_2@C_{78}$ were computed with the hybrid density functional theory at the B3LYP level[22] using the Gaussian 98 program.[23] The standard 6-31G(d) basis set[24] for C and the small-core RECP (relativistic effective core potential) plus valence double-ζ basis set (LanL2DZ)[25] for Ti were employed. Such a combination of basis sets is denoted as DZP. The NMR chemical shielding tensors were evaluated using the gauge-independent atomic orbital (GIAO) method.[26] The geometry of $Ti_2C_2@C_{78}$ used in the GIAO-B3LYP/DZP computation was re-optimized at the B3LYP/DZP level of theory. Based on the computed chemical shielding tensors, theoretical ^{13}C NMR chemical shifts were calculated relative to C_{60} and converted to the TMS (tetramethylsilane) scale using the experimental value for C_{60} (142.5 ppm).[27] This method has proved to be sufficiently accurate at reproducing ^{13}C NMR chemical shifts of several metallofullerenes.[28]

3. RESULTS AND DISCUSSION

3.1. $Ti_2C_2@C_{78}$

In agreement with the previous DFT-B3LYP/6-31G* calculations by Yumura et al.,[10b] the present PBE/DNP calculations predict a ground-state structure **1a** (end-on isomer) and a high-energy isomer **1b** (side-on isomer) for $Ti_2C_2@C_{78}$ (Fig. 1). For the ground-state structure **1a**, the encapsulated Ti_2C_2 cluster has a linear structure with an optimal Ti–C bond length of 1.95 Å. The nearest distance between the Ti atom and D_{3h}-symmetric C_{78} cage is 2.14 Å. Hence, the Ti–C (C_2 moiety) bonding within the Ti_2C_2 is much stronger than the Ti-cage bonding. Notably, the C–C bond length of 1.24 Å for the encapsulated C_2

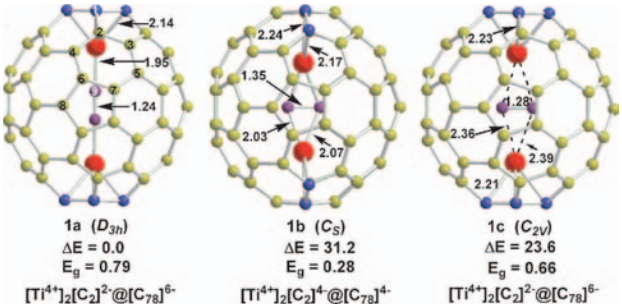

1a (D_{3h}) $\Delta E = 0.0$ $E_g = 0.79$ $[Ti^{4+}]_2[C_2]^{2-}@[C_{78}]^{6-}$

1b (C_S) $\Delta E = 31.2$ $E_g = 0.28$ $[Ti^{4+}]_2[C_2]^{4-}@[C_{78}]^{4-}$

1c (C_{2V}) $\Delta E = 23.6$ $E_g = 0.66$ $[Ti^{4+}]_2[C_2]^{2-}@[C_{78}]^{6-}$

Fig. 1. PBE/DNP-optimized geometries (key atomic distances in Å), relative energies (ΔE, in kcal/mol), HOMO-LUMO gaps (E_g, in eV) and valence states of $Ti_2C_2@C_{78}$ isomers with the C_{78} (D_{3h}) cage. **1a** and **1b** are two local minima confirmed by harmonic vibrational analyses. The Ti atoms are represented by large red balls. The carbon atoms of the encapsulated carbide moiety are purple-colored. The carbon cage atoms are yellow-colored, except those blue-colored ones that are directly connected with the Ti atoms (with C–Ti distances smaller than 2.30 Å).

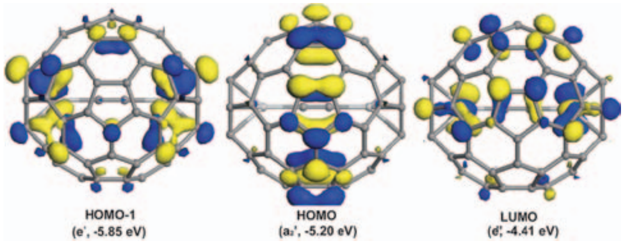

Fig. 2. Isodensity surfaces for the frontier molecular orbitals of $Ti_2C_2@C_{78}$ **1a**.

moiety is typical of a C≡C triple bond,[29] indicating the C_2 moiety is likely an acetyldiide (C_2^{2-}).[30] Indeed, a careful inspection of the Kohn-Sham wavefunction of **1a** reveals that its high-lying occupied molecular orbitals (MOs) are mainly derived from the frontier orbitals of the C_{78}^{6-} and C_2^{2-} fragments, whereas none of them has remarkable contribution from the valence atomic orbitals (3d, 4s, 4p) of Ti atoms. Hence, **1a** has the formal valence state of $[Ti^{4+}]_2[C_2]^{2-}@[C_{78}]^{6-}$ with all its constituents (Ti^{4+}, C_2^{2-} and C_{78}^{6-}) adopting close–shell electronic configurations.[31] The isodensity surfaces for the frontier molecular orbitals (FMOs) of **1a** are depicted in Figure 2. The highest occupied molecular orbital (HOMO) is the 17a_2' MO, which is mainly localized within equatorial area of the C_{78}^{6-} cage. The lowest unoccupied molecular orbitals (LUMOs) are the doubly-degenerate 39e" MOs, which are hybrid of the cage orbital and the orbital of the encase $[Ti_2C_2]^{6+}$ cluster. In addition, the HOMO-1 orbitals (46e′) indicates the dative bonding between d-oribtals of the Ti^{4+} cations and the C_{78}^{6-} cage. The HOMO-LUMO gap (0.79 eV) of **1a** is fortunately close to the observed optical gap (~0.88 eV)[14a] of the previously synthesized Ti_2C_{80}.

For the side-on isomer **1b**, the encapsulated Ti_2C_2 cluster adopts a butterfly-like structure with the Ti–C(C_2 moeity) distances around 2.05 Å, whereas the nearest Ti–C (cage) distances are 2.17 Å. The C–C bond length (1.35 Å) of the encapsulated C_2 unit is typical of a C=C double bond, suggesting the C_2 moiety is an ethyldiide (C_2^{4-}). In accordance with such an assignment, a detailed analysis of the Kohn-Sham wavefunction of **1b** indicates a valence state of $[Ti^{4+}]_2[C_2]^{4-}@C_{78}^{4-}$. Figure 3 depicts the isodensity surfaces of its FMOs. Note that the HOMO-1 (119a") is dominantly localized within the Ti_2C_2 cluster, showing the dative bonding between the d_π-orbitals of the Ti^{4+} cations and the $2\pi^*$-orbital of the C_2^{4-} moiety. Its HOMO(143a′) and LUMO(144a′) are mainly delocalized around the C_{78}^{4-} cage. The HOMO-LUMO gap of **1b** is too narrow (0.28 eV), suggesting this structure is kinetically far less stable than the ground-state structure **1a**. Note that the hollow C_{78}^{4-} (D_{3h}) cage is predicted to have a triplet ground state at the PBE/DNP level. The narrow HOMO-LUMO gap of **1b** can be ascribed to the instability of its C_{78}^{4-} cage. Furthermore, **1b** is by 31.2 kcal/mol higher in energy than the ground state structure **1a** at the PBE/DNP level of theory, comparable to the previous B3LYP/6-31G* prediction of 38.3 kcal/mol. It should be noted that a rather small activation barrier (~10.4 kcal/mol) was predicted by Yumura et al. for the conversion of **1b** to **1a**. Based on these theoretical predictions, it is reasonable to conclude that **1b** is a metastable doubly-excited state of **1a** and can hardly be observed under normal conditions.

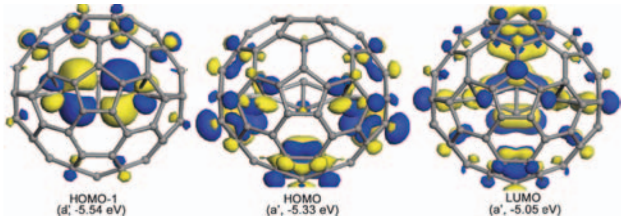

Fig. 3. Isodensity surfaces for the frontier molecular orbitals of $Ti_2C_2@C_{78}$ **1b**.

Table I. Theoretical and experimental ^{13}C NMR chemical shifts (in ppm) of $Ti_2C_2@C_{78}(D_{3h})$.

Theory[a]	Experiment[b]	Site[c]	N_C^d
126.7	129.8	C1	12
129.9	130.5	C2	12
131.2	131.6	C5	6
136.8	136.4	C4	12
138.4	138.9	C6	12
138.7	140.4	C7	12
141.9	141.6	C3	6
144.0	144.3	C8	6
163.6	N/A	C9[e]	2

[a] GIAO-B3LYP/DZP calculation.
[b] Data extracted from Ref. [14a].
[c] See Figure 1 for definition of the carbon sites.
[d] Number of equivalent C atoms.
[e] Acetyldiide carbon.

In addition to **1a** and **1b**, we have also considered a C_{2v}-symmetric isomer **1c** (Fig. 1) which was previously concerned by us at the B3LYP/6-31G* level of theory.[10a] However, the present PBE/DNP calculations reveal that this structure is by 23.6 kcal/mol higher than the ground state structure **1a**, and is a second-order saddle point with two imaginary frequencies by harmonic vibrational analyses. Hence, bending of the C_2 moiety within the linear Ti_2C_2 endohedral cluster is not feasible at room temperature.

The predicted ^{13}C NMR chemical shifts of $Ti_2C_2@C_{78}(D_{3h})$ **1a** are listed in Table I. The theoretical ^{13}C NMR chemical shifts of the C_{78} (D_{3h}) cage range from 126.7 to 144.0 ppm, in reasonable agreement with the experimental ones ranging from 129.8 to 144.3 ppm. For the acetyldiide moiety, the predicted ^{13}C chemical shift is 163.6 ppm, falling into the ^{13}C chemical shift range for fullerene anions.[32] It is not clear why this moiety was not observed in the previous ^{13}C NMR spectroscopic experiments.

3.2. $Zr_2C_2@C_{78}$

The ground-state structure **2a** of $Zr_2C_2@C_{78}$ is depicted in Figure 4. This structure is C_2-symmetric; the Zr_2C_2

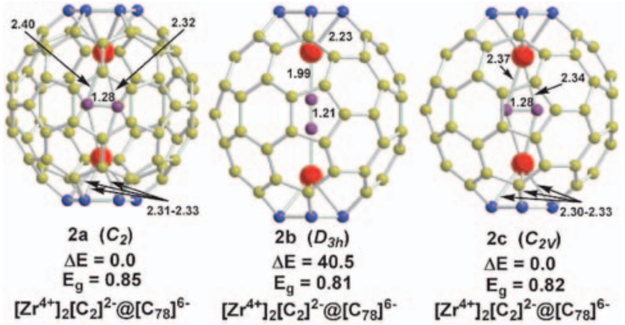

Fig. 4. PBE/DNP-optimized geometries (key atomic distances in Å), relative energies (ΔE, in kcal/mol), HOMO-LUMO gaps (E_g, in eV) and valence states of $Zr_2C_2@C_{78}$ isomers with the C_{78} (D_{3h}) cage. **2a** is the ground-state structure. **2b** and **2c** are transition states. The Zr atoms are represented by large red balls. The carbon atoms of the encapsulated carbide moiety are purple-colored. The carbon cage atoms are yellow-colored, except those blue-colored ones that are directly connected with the Zr atoms (with C-Zr distances smaller than 2.33 Å).

cluster adopts a side-on binding mode encapsulated in the C_{78} (D_{3h}) cage. The optimal Zr-C(C_2 moiety) distances are 2.32 and 2.40 Å, whereas the nearest Zr-C(cage) distances are around 2.31 Å. The optimal C–C bond length of the encapsulated C_2 moiety is 1.28 Å, typical of an acetylide (C_2^{2-}). Based on the Kohn-Sham wave function of **2a**, its valence state can be derived as $[Zr^{4+}]_2[C_2]^{2-}@[C_{78}]^{6-}$, in which all constitents (Zr^{4+}, C_2^{2-}, C_{78}^{6-}) adopt close–shell electronic configurations. As shown in Figure 5, its LUMO is mainly derived from the empty $d_\pi(Zr^{4+})$-$2\pi^*(C_2^{2-})$ bonding orbital of the $[Zr_2C_2]^{6+}$ cluster, whereas its HOMO is localized around the equatorial area of the $C_{78}^{6-}(D_{3h})$ cage. Its HOMO-1 is a hybrid of the d(Zr) orbitals and the orbitals of the $C_{78}^{6-}(D_{3h})$ cage, indicating the dative-bonding between the Zr^{4+} cations and the $C_{78}^{6-}(D_{3h})$ cage. This is reason why the Zr^{4+} cations preferentially locate at the two polar hexgons of the $C_{78}^{6-}(D_{3h})$ cage. The HOMO-LUMO gap (0.85 eV) of $Zr_2C_2@C_{78}$ **2a** is slightly larger than the HOMO-LUMO gap (0.79 eV) of $Ti_2C_2@C_{78}$ **1a**, suggesting both metal-carbide endofullerene should have like kinetical stability. Hence, $Zr_2C_2@C_{78}$ should be as synthetically approachable as $Ti_2C_2@C_{78}$.

In addition to the ground-state structure **2a**, two transitions states **2b** and **2c** (Fig. 4) have also been located in our calculations. In **2b**, the encapsulated Zr_2C_2 cluster adopts a linear end-on binding mode, similar to the Ti_2C_2 cluster in the the ground-state structure of $Ti_2C_2@C_{78}$. **2b** is a transition state responsible for the rotation of the C_2 moiety within the Zr_2C_2 plane. However, such a rotation is kinetically forbidden at room temperature on account of the large activation energy (40.5 kcal/mol) required. On the contrary, the rotation of the C_2 moiety around the C_3-axis of the C_{78} cage appears to be barrierless; the transition state **2c** responsible for such a rotation is *nearly isoenergetic* with the ground-state structure **2a** at the PBE/DNP level.

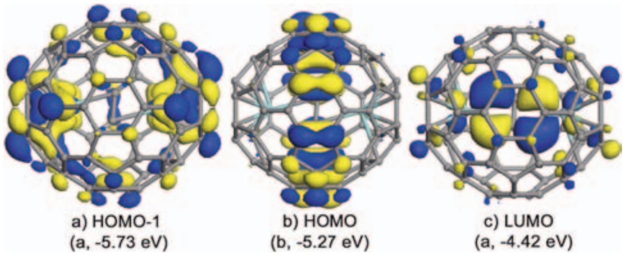

Fig. 5. Isodensity surfaces for the frontier molecular orbitals of $Zr_2C_2@C_{78}$ **2a**.

3.3. $Hf_2C_2@C_{78}$

As shown in Figure 6, our PBE/DNP calculations predicted two isoenergetic isomers **3a** and **3b** as the ground-state structure of $Hf_2C_2@C_{78}$. Hence, rotation of the encapsulated C_2 moiety around the C_3-axis of the C_{78} cage

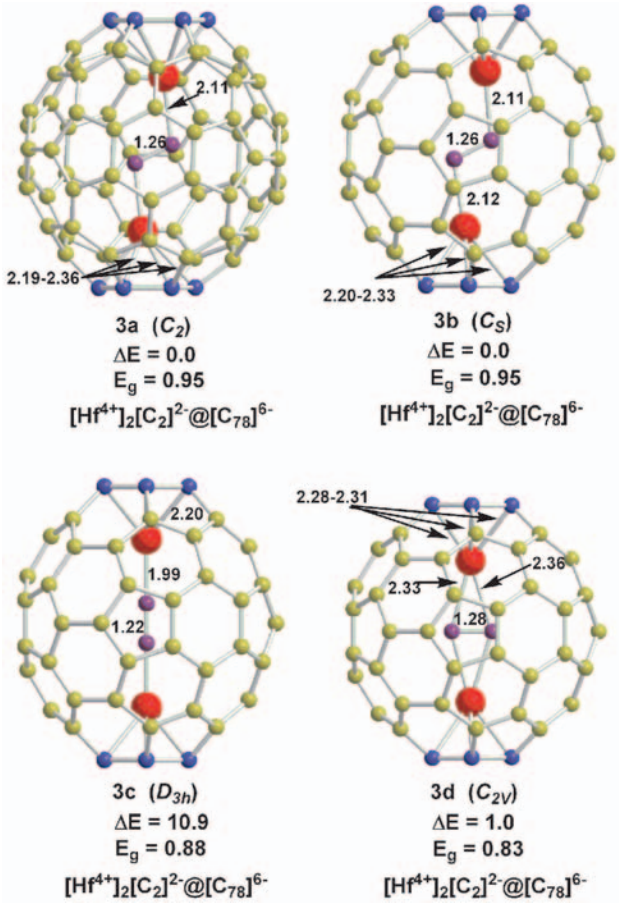

Fig. 6. PBE/DNP-optimized geometries (key atomic distances in Å), relative energies (ΔE, in kcal/mol), HOMO-LUMO gaps (E_g, in eV) and valence states of $Hf_2C_2@C_{78}$ isomers with the C_{78} (D_{3h}) cage. **3a** and **3b** are two local minima confirmed by harmonic vibrational analyses. The Hf atoms are represented by large red balls. The carbon atoms of the encapsulated carbide moiety are purple-colored. The carbon cage atoms are yellow-colored, except those blue-colored ones that are directly connected with the Hf atoms (with C–Hf distances smaller than 2.36 Å).

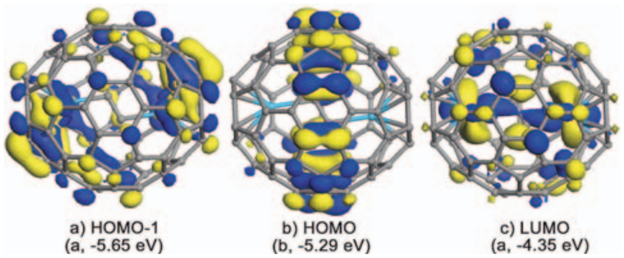

Fig. 7. Isodensity surfaces for the frontier molecular orbitals of $Hf_2C_2@C_{78}$ **3a**.

Table II. Ionic radii (in Å) for 6-coordinated M^{4+} (M = Ti, Zr, Hf) and the pole-pole distances (R_{pp}, in Å) of the C_{78}^{6-} (D_{3h}) cages in the $M_2C_2@C_{78}$ (M = Ti, Zr, Hf) containing a linear $[M_2C_2]^{6+}$ cluster.

M	Ionic radii[a, b]	Structure	R_{pp}
Ti	0.61(6), 0.74(8)	$Ti_2C_2@C_{78}$ **1a**	8.25
Zr	0.72(6), 0.84(8)	$Zr_2C_2@C_{78}$ **2b**	8.47
Hf	0.71(6), 0.83(8)	$Hf_2C_2@C_{78}$ **3c**	8.42

[a] Data extracted from Ref. [29].
[b] The coordination numbers of the cations are given in parentheses.

should be very fast at the room temperature. Both isomers **3a** and **3b** have the valence state $[Hf^{4+}][C_2]^{2-}@[C_{78}]^{6-}$. The predicted close–shell electronic configuration of $Hf_2C_2@C_{78}$ is in line with the previously observed diamagneticity of Hf_2C_{80}.[18] The predicted HOMO-LUMO gaps (0.95 eV) for both isomers luckily agree well with the optical gap (0.95 eV)[18] of Hf_2C_{80} measured by UV-Vis-NIR absorption spectroscopy, but slightly larger than those of the congeneric $M_2C_2@C_{78}$ (M = Ti, Zr). The encapsulated Hf_2C_2 cluster in both isomers adopts a zigzag geometry with the nearest Hf-C(C_2 moiety) distances of 2.11 Å, slightly longer than the nearest Hf-C(cage) distance (~2.20 Å). The C–C bond length of the C_2^{2-} moiety is 1.26 Å.

Since both isomers have like electronic structure, only the FMOs of $Hf_2C_2@C_{78}$ **3a** are depicted in Figure 7 for discussion. The composition of the HOMO-1, HOMO, and LUMO for $Hf_2C_2@C_{78}$ **3a** (Fig. 7) is quite similar to that of $Zr_2C_2@C_{78}$ **2a** (Fig. 5). Its HOMO-1 shows the dative-bonding between the d(Hf^{4+}) orbital and the cage (C_{78}^{6-}) orbital, whereas its HOMO is mainly delocalized around the equatorial area of the C_{78}^{6-} cage. The LUMO is mainly due to d(Hf^{4+}) orbitals and $2\pi^*(C_2^{2-})$ orbital with minor contribution from the orbital of C_{78}^{6-} cage.

The optimized geometries of two other possible isomers, **3c** and **3d**, of $Hf_2C_2@C_{78}$ are also depicted in Figure 6. The D_{3h}-symmetric isomer **3c** containing a linear Hf_2C_2 cluster is a saddle point by 10.9 kcal/mol higher than isomers **3a/3b**. The C_{2V}-symmetric isomer **3d** is by only 1.0 kcal/mol higher than isomers **3a/3b**, and is a transition sate responsible for in-plane waging of the C_2^{2-} moiety between two Hf^{4+} cations that leads to the interconversion of two equivalent isomers **3b**.

At this stage, it is interesting to note that for this series of congeneric endofullerenes $M_2C_2@C_{78}$ (M = Ti, Zr, Hf), the linear endohedral cluster $[M_2C_2]^{6+}$ is stable for M = Ti (structure **1a**), but becomes unstable for M = Zr (structure **2b**) and Hf (structure **3c**). Table II lists the radii of M^{4+} (M = Ti, Zr, Hf) and the pole–pole distances of the C_{78}^{6-} (D_{3h}) cages in the structures **1a**, **2b**, and **3c**. Since the radii of Zr^{4+} and Hf^{4+} are much larger than that of Ti^{4+}, accommodating a linear $[M_2C_2]^{6+}$ cluster in the C_{78}^{6-} (D_{3h}) cage should exert larger steric strain onto the carbon cage for M = Zr and Hf than for M = Ti. This is evidenced by the much longer polar–polar distances of the C_{78}^{6-} (D_{3h}) cages in $Zr_2C_2@C_{78}$ **2b** and $Hf_2C_2@C_{78}$ **3c** than in $Ti_2C_2@C_{78}$ **1a**. In addition, the ground-state structure of the heavier $M_2C_2@C_{78}$ (M = Zr, Hf) adopts the side-on (for $Zr_2C_2@C_{78}$**2a**) and zig-zag (for $Hf_2C_2@C_{78}$ **3a** or **3b**) geometries, respectively. Such a difference may be due to (i) Hf^{4+} is slightly smaller than Zr^{4+} (c.f. Table II), and (ii) Hf^{4+} is more electrophilic than Zr^{4+}; Hf^{4+} (in **3a** or **3b**) is thus closer to the electron-rich C_2^{2-} moiety and to the C_{78}^{6-} cage by adopting the zig-zag geometry.

3.4. Electronic Properties of $M_2C_2@C_{78}$(M = Ti, Zr, Hf)

We have computed the monocations and monoanions of $M_2C_2@C_{78}$ (M = Ti, Zr, Hf) to derive their redox properties such as their gas-phase ionization potentials (IPs) and electron affinities (EAs). The predicted data are listed in Table III. The FMOs for $M_2C_2@C_{78}$ (M = Ti, Zr, Hf) shown in Figures 2, 5, and 7 are indicative of their redox properties. For $Ti_2C_2@C_{78}$ **1a**, both its HOMO and LUMO are mainly delocaized around the C_{78}^{6-} cage (Fig. 2). Accordingly, its monoanion and monocation have the valence states $[Ti^{4+}]_2[C_2]^{2-}@C_{78}^{7-}$ and $[Ti^{4+}]_2[C_2]^{2-}@C_{78}^{5-}$, respectively; the C_2^{2-} moiety is unchanged in such one-electron processes. For $Zr_2C_2@C_{78}$ **2a** and $Hf_2C_2@C_{78}$ **3a**, their HOMOs are also delocalized around the C_{78}^{6-} cage (see Figs. 5 and 7). The valence states for their monocations are $[M^{4+}]_2[C_2]^{2-}@C_{78}^{5-}$ (M = Zr, Hf). On the contrary, their LUMOs are due primarily to the empty d(Hf^{4+})-$2\pi^*(C_2^{2-})$ bonding orbital. As a result, their monoanions have the valence states $[M^{4+}]_2[C_2]^{3-}@C_{78}^{6-}$ (M = Zr, Hf), in which the C–C bond of the encapsulated C_2 moiety is elongated from 1.28/1.26 for neutral ones (**2a**/**3a**) to 1.31/1.32 Å for the monoanions (**2a**$^-$/**3a**$^-$).

From Table III, the computed IPs for the $M_2C_2@C_{78}$ (M = Ti, Zr, Hf) follow the order: $Ti_2C_2@C_{78} < Hf_2C_2@C_{78} \ll Zr_2C_2@C_{78}$, whereas the order for the predicted EAs is $Ti_2C_2@C_{78} < Hf_2C_2@C_{78} \approx Zr_2C_2@C_{78}$. Hence, $Zr_2C_2@C_{78}$ is as reducible as $Hf_2C_2@C_{78}$, but far less oxidizable than $Hf_2C_2@C_{78}$ and $Ti_2C_2@C_{78}$, meaning that the overall chemical reactivity of $Zr_2C_2@C_{78}$ is lower than that of $Hf_2C_2@C_{78}$. Since both $Hf_2C_2@C_{78}$ and $Ti_2C_2@C_{78}$ have been synthesized and isolated

Table III. PBE/DNP-predicted ionization potentials (IP, in eV) and electron affinities (EA, in eV) for the $M_2C_2@C_{78}$ (M = Ti, Zr, Hf), the valence states (VS) of their monoanions and monocations and the bond-length of encapsulated C_2 moiety (R_{CC} in Å).

	$Ti_2C_2@C_{78}$		$Zr_2C_2@C_{78}$		$Hf_2C_2@C_{78}$	
	1a$^+$	**1a**$^-$	**2a**$^+$	**2a**$^-$	**3a**$^+$	**3a**$^-$
R_{cc}	1.24	1.24	1.28	1.31	1.26	1.32
VS	$[Ti^{4+}]_2C_2^{2-}@C_{78}^{5-}$	$[Ti^{4+}]_2C_2^{2-}@C_{78}^{7-}$	$[Zr^{4+}]_2C_2^{2-}@C_{78}^{5-}$	$[Zr^{4+}]_2C_2^{3-}@C_{78}^{6-}$	$[Hf^{4+}]_2C_2^{2-}@C_{78}^{5-}$	$[Hf^{4+}]_2C_2^{3-}@C_{78}^{6-}$
IP^a	6.54		7.40		6.62	
EA^b	3.00		3.41		3.40	

^{a}IP = $E[(M_2C_2@C_{78})^+] - E[M_2C_2@C_{78}]$.
^{b}EA = $E[M_2C_2@C_{78}] - E[(M_2C_2@C_{78})^-]$

successfully,[14a,18] we believe $Zr_2C_2@C_{78}$ is synthetically approachable. From the IPs and EAs listed in Table III, we may expect that the reactivity of these endofullerenes toward an electrophilic reagent would follow the order $Ti_2C_2@C_{78} > Hf_2C_2@C_{78} \gg Zr_2C_2@C_{78}$, whereas the order of their reactivity toward a nucleophilic reagent would be $Ti_2C_2@C_{78} < Hf_2C_2@C_{78} \approx Zr_2C_2@C_{78}$.

4. CONCLUDING REMARKS

We have conducted a systematic DFT investigation on the structures and electronic properties of the metal-carbide endofullerenes $M_2C_2@C_{78}$ (M = Ti, Zr, Hf) at the PBE/DNP level of theory. It is shown that this series of endofullerenes have the valence states $[M^{4+}]_2C_2^{2-}@C_{78}^{6-}$ that follow faithfully the stable close–shell electronic configuration rule,[2–4] and are rational structural models for the previously synthesized M_2C_{80} (M = Ti, Hf).[14a,18] The structure of the $[M_2C_2]^{6+}$ cluster encapsulated in the $C_{78}^{6-}(D_{3h})$ cage varies with the increasing of the ionic radius of M^{4+}, i.e., from a linear M–C ≡ C–M geometry for M = Ti, through a zigzag geometry for M = Hf to a side-on binding mode for M = Zr. Among the three endofullerenes, the two heavier ones, $M_2C_2@C_{78}$ (M = Zr, Hf), should display interesting intramolecular dynamic behavior at room temperature, i.e., the encapsulated C_2^{2-} moiety can rotate freely around the C_3-axis of the C_{78}^{6-} (D_{3h}) cage. For the lightest one ($Ti_2C_2@C_{78}$), the encapsulated $[Ti_2C_2]^{6-}$ is far more fixed by adopting the linear Ti–C ≡ C–Ti geometry.

Finally, the computed redox properties such as the gas-phase ionization potentials and electron affinities of these endofullerenes suggest that $Zr_2C_2@C_{78}$ is as viable as the previously synthesized $Hf_2C_2@C_{78}$.

Acknowledgments: This work was sponsored by NSFC (Grants No. 20021002, 20425312, 20203013, 20423002, 90206038), MOE of China (Grant No. 20010384005), Fok Ying-Tung Education Foundation, NSF of Fujian Province (Grants No. E0210001 and 2002F010) and Xiamen University through the Minjiang Professorship. We thank Dr. Z. Chen for insightful discussions.

References and Notes

1. H. Shinohara, *Rep. Prog. Phys.* 63, 843 (**2000**).
2. (a) D. M. P. Mingos, T. Slee, and Z. Lin, *Chem. Rev.* 90, 383 (**1990**); (b) D. M. P. Mingos and D. J. Wales, Introduction to Cluster Chemistry, Prentice-Hall, Englewood Cliffs, NewJersey (**1990**).
3. (a) H. W. Kroto, *Nature* 329, 529 (**1987**); (b) P. W. Fowler, *J. Phys. Chem. Solids* 54, 1825 (**1993**); (c) M. F. Fan, Z. Lin, and S. Yang, *J. Mol. Struct. -Theochem.* 337, 231 (**1995**); (d) P. W. Fowler and F. Zerbetto, *Chem. Phys. Lett.* 243, 36 (**1995**).
4. X. Lu and Z. Chen, *Chem. Rev*. 105, 3643 (**2005**).
5. Y. Maeda, J. Miyashita, T. Hasegawa, T. Wakahara, T. Tsuchiya, L. Feng, Y. Lian, T. Akasaka, K. Kobayashi, S. Nagase, M. Kako, K. Yamamoto, and K. M. Kadish, *J. Am. Chem. Soc.* 127, 2143 (**2005**).
6. (a) C.-R. Wang, T. Kai, T. Tomiyama, T. Yoshida, Y. Kobayashi, E. Nishibori, M. Takata, M, Sakata, and H. Shinohara, *Nature* 408, 426 (**2000**); (b) M. Takata, E. Nishibori, C.-R. Wang, M. Sakata, and H. Shinohara, *Chem. Phys. Lett.* 372, 512 (**2003**).
7. (a) S. Stevenson, P. W. Fowler, T. Heine, J. C. Duchamp, G. Rice, T. Glass, K. Harich, E. Hajdu, R. Bible, and H. C. Dorn, *Nature* 408, 428 (**2000**); (b) M. M. Olmstead, H. M. Lee, J. C. Duchamp, S. Stevenson, D. Marciu, H. C. Dorn, and A. L. Balch, *Angew. Chem. Int. Ed.* 42, 900 (**2003**).
8. Z.-Q. Shi, X. Wu, C.-R. Wang, X. Lu, and H. Shinohara, *Angew. Chem. Int. Ed.* 45, 2107 (**2006**).
9. H. Kato, A. Taninaka, T. Sugai, and H. Shinohara, *J. Am. Chem. Soc.* 125, 7782 (**2003**).
10. (a) K. Tan and X. Lu, *Chem. Commun.* 4444 (**2005**); (b) T. Yumura, Y, Sato, K. Suenaga, and S. Iijima, *J. Phys. Chem. B* 109, 20251 (**2005**).
11. (a) Y. Iiduka, T. Wakahara, T. Nakahodo, T. Tsuchiya, A. Sakuraba, Y. Maeda, T. Akasaka, K. Yoza, E. Horn, T. Kato, M. T. H. Liu, N. Mizorogi, N. Kobayashi, and T. Nagase, *J. Am. Chem. Soc.* 127, 12500 (**2005**); (b) K. Tan and X. Lu, *J. Phys. Chem. A* 110, 1176 (**2006**).
12. K. Tan, X. Lu, and C.-R. Wang, unpublished results.
13. (a) M. M. Olmstead, A. de Bettencourt-Dias, J. C. Duchamp, S. Stevenson, D. Marciu, H. C. Dorn, and A. L. Balch, *Angew. Chem., Int. Ed.* 40, 1223 (**2001**); (b) S. Stevenson, G. Rice, T. Glass, K. Harich, F. Croner, M. R. Jordan, J. Craft, E. Hadju, R. Bible, M. M. Olmstead, K. Maitra, A. J. Fisher, A. L. Balch, and H. C. Dorn, *Nature* 401, 55 (**1999**); (c) B. Cao, T. Wakahra, T. Tsuchiya, M. Kondo, Y. Maeda, G. M. Aminur Rahman, T. Akasaka, K. Kobayashi, S. Nagase, and K. J. Yamamoto, *J. Am. Chem. Soc.* 126, 9164 (**2004**); (d) H. Shimotani, T. Ito, Y. Iwasa, A. Taninaka, H. Shinohara, E. Nishibori, M. Takata, and M. Sakata, *J. Am. Chem. Soc.* 126, 364 (**2004**); (e) T. Akasaka, S. Nagase, K. Kobayashi, M. Wälchli, K. Yamamoto, H. Funasaka, M. Kako, T. Hoshino, and T. Erata, *Angew. Chem. Int. Ed.* 36, 1643 (**1997**).
14. (a) B. Cao, M. Hasegawa, K. Okada, T. Tomiyama, T. Okazaki, K. Suenaga, and H. Shinohara, *J. Am. Chem. Soc.* 123, 9679 (**2001**);

(b) R. Jaffiol, A. Débarre, C. Julien, D. Nutarelli, P. Téchnio, A. Taninaka, B. Cao, T. Okazaki, and H. Shinohara, *Phys. Rev. B* 68, 14105 (**2003**); (c) K. Iwasaki, S. Hino, D. Yoshimura, B. Cao, T. Okazaki, and H. Shinohara, *Chem. Phys. Lett.* 397, 169 (**2004**); (d) S. Hino, K. Iwasaki, D. Wanita, D. Yoshimura, B. Cao, T. Okazaki, and H. Shinohara, *Fullerenes, Nanotubes, Carbon Nanostruct.* 12, 33 (**2004**).

15. (a) H. Shinohara, H. Sato, M. Ohkohchi, Y. Ando, T. Kodama, T. Shida, T. Kato, and Y. Saito, *Nature* 357, 52 (**1992**); (b) C. S. Yannoni, M. Hoinkis, M. S. D. Vries, D. S. Bethune, I. R. Salem, M. S. Crowder, and R. D. Johnson, *Science* 256, 1191 (**1992**); (c) M. Takata, E. Nishibori, M. Sakata, M. Inakuma, E. Yamamoto, and H. Shinohara, *Phys. Rev. Lett.* 83, 2214 (**1999**).

16. (a) B. Cao, K. Suenaga, T. Okazaki, and H. Shinohara, *J. Phys. Chem. B* 106, 9295 (**2004**); (b) K. Sueki, K. Kikuchi, K. Akiyama, T. Sawa, M. Katada, S. Ambe, F. Ambe, and H. Nakahara, *Chem. Phys. Lett.* 300, 140 (**1999**).

17. (a) C.-R. Wang, T. Kai, T. Tomiyama, T. Yoshida, Y. Kobayashi, E. Nishibori, M. Takata, M. Sakata, and H. Shinohara, *Angew. Chem. Int. Ed.* 40, 397 (**2001**); (b) M. Krause, M. Hulman, H. Kuzmany, O. Dubay, G. Kresse, G. Seifert, C. Wang, and H. Shinohara, *Phys. Rev. Lett.* 93, 137403 (**2004**).

18. K. Akiyama, K. Sueki, T. Kodama, K. Kikuchi, Y. Takigawa, H. Nakahara, I. Ikemoto, and M. Katada, *Chem. Phys. Lett.* 317, 490 (**2000**).

19. J. P. Perdew, K. Burke, and M. Ernzerhof, *Phys. Rev. Lett.* 77, 3865 (**1996**).

20. (a) B. Delley, *J. Chem. Phys.* 92, 508 (**1990**); (b) B. Delley, *J. Chem. Phys.* 113, 7756 (**2000**).

21. (a) M. Douglas and N. M. Kroll, *Acta Phys.* 82, 89 (**1974**); (b) D. D. Koelling and B. N. Harmon, *J. Phys. C: Solid State Phys.* 10, 3107 (**1977**).

22. (a) A. D. Becke, *J. Chem. Phys.* 98, 5648 (**1993**); (b) C. Lee, W. Yang, and R. G. Parr. *Phys. Rev. B* 37, 785 (**1988**).

23. M. J. Frisch, G. W. Trucks, H. B. Schlegel, G. E. Scuseria, M. A. Robb, J. R. Cheeseman, V. G. Zakrzewski, J. A. Montgomery, Jr., R. E. Stratmann, J. C. Burant, S. Dapprich, J. M. Millam, A. D. Daniels, K. N. Kudin, M. C. Strain, O. Farkas, J. Tomasi, V. Barone, M. Cossi, R. Cammi, B. Mennucci, C. Pomelli, C. Adamo, S. Clifford, J. Ochterski, G. A. Petersson, P. Y. Ayala, Q. Cui, K. Morokuma, D. K. Malick, A. D. Rabuck, K. Raghavachari, J. B. Foresman, J. Cioslowski, J. V. Ortiz, A. G. Baboul, B. B. Stefanov, G. Liu, A. Liashenko, P. Piskorz, I. Komaromi, R. Gomperts, R. L. Martin, D. J. Fox, T. Keith, M. A. Al-Laham, C. Y. Peng, A. Nanayakkara, C. Gonzalez, M. Challacombe, P. M. W. Gill, B. G. Johnson, W. Chen, M. W. Wong, J. L. Andres, M. Head-Gordon, E. S. Replogle, and J. A. Pople, GAUSSIAN 98 (Revision A.11), Gaussian, Inc., Pittsburgh, PA (**1998**).

24. W. J. Hehre, R. Ditchfield, and J. A. Pople, *J. Chem. Phys.* 56, 2257 (**1972**).

25. P. J. Hay and W. R. Wadt, *J. Chem. Phys.* 82, 299 (**1985**).

26. K. Wolinski, J. F. Hilton, and P. J. Pulay, *J. Am. Chem. Soc.* 112, 8251 (**1990**).

27. (a) R. Taylor, J. P. Hare, A. K. Abdul-Sada, and H. W. Kroto, *J. Chem. Soc., Chem. Commun.* 1423 (**1990**); (b) R. Taylor, G. J. Langley, A. G. Avent, T. J. S. Dennis, H. W. Kroto, and D. R. M. Walton, *J. Chem. Soc. Perkin Trans.* 2, 1029 (**1993**).

28. (a) J. C. Duchamp, A. Demortier, K. R. Fletcher, D. Dorn, E. B. Iezzi, T. Glass, and H. C. Dorn, *Chem. Phys. Lett.* 375, 655 (**2003**); (b) K. Kobayashi and S. Nagase, *Chem. Phys. Lett.* 362, 373 (**2003**).

29. J. A. Dean, Lange's handbook of chemistry, McGram-Hill. Inc. (**1999**), 15th edn.

30. (a) R. B. King, *J. Organomet. Chem.* 536/537, 7 (**1997**); (b) F. A. Cotton, G. C. Wilkinson, A. Murillo, and M. Bochmann, Advanced Inorganic Chemistry, Wiley-Interscience, New York (**1999**), p. 221, 6th edn.

31. PBE/DNP calculations reveal that C_{78}^{6-} (D_{3h}) favors a close–shell electronic configuration with a HOMO-LUMO gap of ~1.32 eV, whereas the tetraanion C_{78}^{4-} (D_{3h}) favors a triplet ground state.

32. C. A. Reed and R. D. Bolskar, *Chem. Rev.* 100, 1075 (**2000**).

Received: 26 January 2006. Revised/Accepted: 16 April 2006.